ACADÉMIE
DES SCIENCES
INSTITUT DE FRANCE

Comptes Rendus

Géoscience

Sciences de la Planète

Benoît Joseph Mbassa, Jesús Solé, Daouda Dawaï, Caroline Ngwa Neh, Zénon Itiga, Jean-Paul Sep Nlomngan, Patrice Augustin Moussango Ibohn, Moïse Bessong, Vincent Ngako and Emmanuel Njonfang

New K–Ar data in the northeastern edge of the Adamawa-Yadé domain, Central African Pan-African Fold Belt: shedding light on the transition age between convergent and divergent tectonic regimes

Volume 357 (2025), p. 145-165

Online since: 10 June 2025

https://doi.org/10.5802/crgeos.289

The Comptes Rendus. Géoscience — Sciences de la Planète *are a member of the Mersenne Center for open scientific publishing*
www.centre-mersenne.org — e-ISSN : 1778-7025

ACADÉMIE DES SCIENCES
INSTITUT DE FRANCE

Comptes Rendus. Géoscience — Sciences de la Planète
2025, Vol. 357, p. 145-165
https://doi.org/10.5802/crgeos.289

Research article
Tectonics, tectonophysics, geodynamics

New K–Ar data in the northeastern edge of the Adamawa-Yadé domain, Central African Pan-African Fold Belt: shedding light on the transition age between convergent and divergent tectonic regimes

Benoît Joseph Mbassa [*, a], **Jesús Solé** [b], **Daouda Dawaï** [c], **Caroline Ngwa Neh** [a], **Zénon Itiga** [d], **Jean-Paul Sep Nlomngan** [a], **Patrice Augustin Moussango Ibohn** [a], **Moïse Bessong** [a], **Vincent Ngako** [a] **and Emmanuel Njonfang** [e]

[a] Institute for Geological and Mining Research, PO Box 4110, Yaoundé, Cameroon

[b] Instituto de Geología, Laboratorio Nacional de Geoquímica y Mineralogía, Universidad Nacional Autónoma de México. 04510 Mexico City, Mexico

[c] Department of Earth Sciences, Faculty of Sciences, University of Maroua, PO Box 814 Maroua, Cameroon

[d] Department of Earth Sciences, University of Douala, PO Box 24157 Douala, Cameroon

[e] Higher Teachers Training School, University of Yaoundé I, member of the Cameroon Academy of Sciences, PO Box 812 Yaoundé, Cameroon

E-mail: benjo_mbassa@yahoo.fr (B. J. Mbassa)

Abstract. The tectonic evolution of the Central African Pan-African Fold Belt in Cameroon has been intensively studied during the last two decades. However, the timing of the last stages of the Pan-African orogenic cycle is still not well constrained, thus leading to controversial interpretations. The present work provides new insights into the late Pan-African tectonic evolution of the Adamawa-Yadé domain. It includes a complex crustal assemblage of the Central African Pan-African Fold Belt, which has undergone a polycyclic evolution since the Palaeoproterozoic. We infer the late Pan-African events of this domain from in-situ dating of biotite in five thin sections of plutonic rocks. The dated rocks are calc-alkaline metaluminous to weakly peraluminous I-type granitoids, consisting of Qz-monzonites and granites, medium- to high-potassic, with shoshonitic affinities, all displaying adakitic signature. The ages obtained were correlated with the available geochronological data for rocks from post-collision events of the Adamawa-Yadé domain and the Central African and Brazilian orogenic belts. The new biotite age range spans 67 Myr geological history of the studied area, from Ediacaran (549 ± 19 Ma) to Early Ordovician (482 ± 6 Ma), which marks the transition between convergent and extensional tectonics regimes in the Central African Pan-African Fold Belt.

Keywords. In-situ K–Ar dating, Central African Pan-African Fold Belt, Adamawa-Yadé domain, Ediacaran, Early Ordovician, Post-collision events.

Manuscript received 19 November 2024, revised 8 March 2025 and 18 March 2025, accepted 20 March 2025.

* Corresponding author

1. Introduction

The main geological units in Cameroon consist of Archean to Late Proterozoic plutonic–metamorphic basement, intruded by Palaeozoic to Mesozoic post-Pan-African terranes and anorogenic plutonic complexes, and partially covered with Cenozoic to Quaternary volcano-sedimentary rocks. The basement includes the northern edge of the Archean Congo craton known as the Ntem complex, the Nyong Palaeoproterozoic unit, and the widespread Central African Pan-African Fold Belt (CAPFB). The geodynamic evolution of the Cameroonian segment of this CAPFB has been the subject of numerous models (e.g. Toteu, Penaye, et al., 2004; Bouyo Houketchang et al., 2009; Ngako and Njonfang, 2011); however, a recent one by Toteu, De Wit, et al. (2022), taking into account petrological and geochronological data together with structural analyses, involves two subductions and four main steps. The successive phases consist of: (1) the break-up and basin development both on the Ntem complex and on the northern and southern limits of the Adamawa-Yadé domain, synchronously with the expansion of the Poli-Leré arc (Tonian—620 Ma); (2) the ubiquitous pre-tectonic plutonism (800–620 Ma); (3) the collisional phase (~620 Ma) was marked by a granulite facies metamorphism in all areas at 600 Ma; and (4) the ultimate one resulting in: (i) the overlapping of the Yaoundé-Yangana units onto the Ntem complex, (ii) the accretion of the Poli-Leré arc to Adamawa-Yadé domain, (iii) the extensive syntectonic magmatism partially controlled by local shear zones (600–580 Ma), and (iv) the emplacement of the Adamawa-Yadé and Poli-Leré post-tectonic granitoids (~550 Ma). The Adamawa-Yadé domain (including our study area) represents an asymmetric band of Precambrian basement rocks located East of the Tcholliré-Banyo shear zone (TBSZ) and extending from Cameroon (Adamawa) to the Central African Republic (Yadé) and even to central Southern Chad (Shellnutt et al., 2020; Djerossem et al., 2021). It comprises Neoproterozoic granitoids emplaced during successive orogenic phases (Delor et al., 2021; Bernard et al., 2019) in a metamorphosed basement. This basement underwent two orogenic cycles: the Eburnean–Transamazonian around 2.1 Ga, then the Pan-African one around 600 Ma (Tanko Njosseu et al., 2005). As much as the Neo-Proterozoic events of the North equatorial Pan-African fold belt are sufficiently described and dated, little is said about its Paleozoic events.

The Palaeozoic Pan-African crustal evolution is marked by an extensional tectonic episode characterised at their early stages by tectonic, geophysical, and structural markers of block readjustments (such as normal faults, horsts, grabens, rifts, etc.), except in the case of aborted rifts. The Late Palaeozoic to Mesozoic tectonic regime of West–Central Africa was ruled by tensional stresses resulting from the reactivation of the Central Africa Shear Zone (Guiraud and Maurin, 1991; Moreau et al., 1987; Tchouankoué et al., 2014) or St. Helena mantle plume activity (Coulon et al., 1996) and accompanied with magmatism (Maluski et al., 1995). Nevertheless, the post-Pan-African magmatism of the CAPFB in Central Africa, particularly the Palaeozoic to Mesozoic magmatism in Cameroon, is still poorly known, although it is of great interest to understand the whole Pan-African orogeny. In this paper, we present evidence of early Palaeozoic events through new K–Ar ages obtained on biotite from magmatic rocks carried out in an area located East of Ngaoundéré city and bounded by the latitudes 7°19′ to 7°45′ North and the longitudes 13°30′ to 14°20′ East (Figure 1c). Their implications on the post-Pan-African evolution of the CAPFB in Cameroon as well as their geodynamic significance (transition between convergent and extensional tectonic regimes) are discussed.

2. Geological setting and review of previous dating results

The regional geology includes Neoproterozoic igneous suites (Linté-Godé, Yangba-Kogué, calc-alkaline suite of central Cameroon), and a vast basalt plateau crosscut by felsic domes in the southeastern region. The basement is underlain by gneisses and syn-to post-tectonic calc-alkaline granitoids, locally covered with volcanic and sedimentary rocks (Toteu, Van Schmus, et al., 2001; Tchameni et al., 2006; Ganwa et al., 2008). The volcanic sequence consists of mafic or felsic lavas resulting from the melt of a heterogeneous mantle, with possible crustal contamination (Nkouandou et al., 2008; Itiga et al., 2014; Tiabou et al., 2018).

The local tectonic is characterised by: (1) the presence of NE–SW mylonitic foliation associated with the regional-scale TBSZ, known as the last stage of a

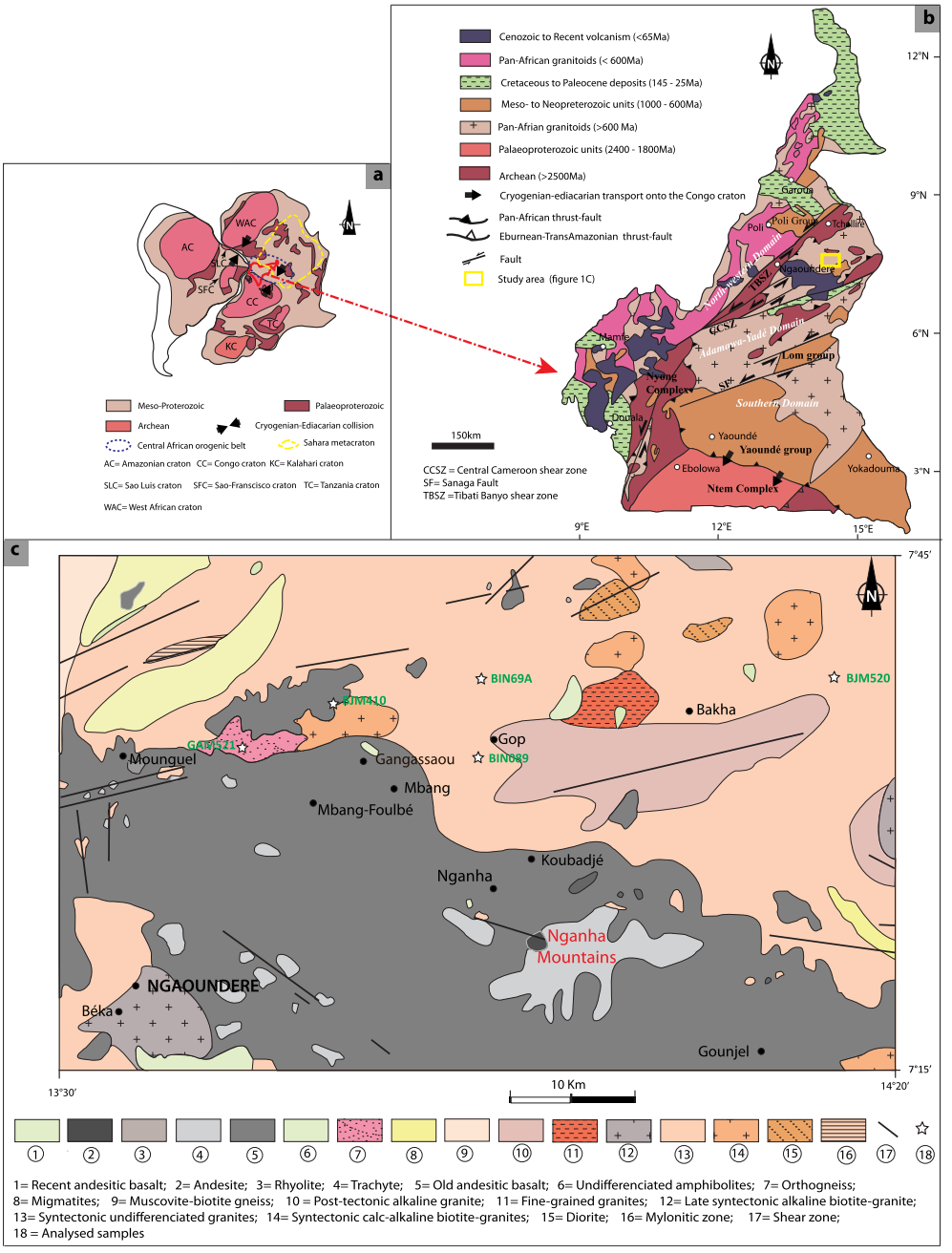

Figure 1. Location of the study area: (a) South America–Africa fit, showing cratons of western Gondwana (modified after Neves et al., 2016); (b) Geological sketch of Cameroon (modified after Castaing et al., 1994; Ngako, Affaton, Nnangue, et al., 2003; Owona et al., 2013) with position of the study area; (c) Simplified geological map of the study area (modified from Lasserre, 1961) together with the position of the studied samples.

D_1–D_2 polyphase deformation associated with high-grade metamorphism that affected the Palaeoproterozoic relics of granulitic assemblages and late tectonic granitoids (Toteu, Van Schmus, et al., 2001; Bouyo Houketchang et al., 2009); and (2) the WSW–ENE dextral Central Cameroon Shear Zone. Nkono et al. (2009) mentioned two main directions of lineaments: (i) The N65E corresponding to the Cenozoic faults, which have controlled the setting up of the Adamawa plateau, and (ii) the N167E direction. This local tectonic was segmented into four phases (D_1 to D_4) of deformation using together structural markers and geochronological data (U–Pb and Sm–Nd dating) (Toteu, Van Schmus, et al., 2001; Toteu, Penaye, et al., 2004; Ngako, Affaton and Njonfang, 2008; Ngako and Njonfang, 2011); D_1 and D_2 mark the crustal thickening event dated between 635–615 Ma. D_1 is represented by a low-dipping syn-migmatitic foliation (S_1) ascribed to the development of nappes oriented towards the East, whereas D_2 corresponds to the transposition of S_1 into conjugate steeply dipping shear zones and upright folds leading to the expansion of the main NE–SW foliation recording the local NW–SE shortening. The D_3 phase dated between 600–580 Ma (U–Pb age; Penaye et al., 1989; Toteu, Van Schmus, et al., 2001) is expressed by deformations along sinistral shear zones trending N–S to NE–SW (e.g. Tcholliré-Banyo) while the D_4 corresponds to a regression associated with the activation of NNE–SSW to E–W dextral shear zones (e.g. CCSZ) around 545 Ma (Bessoles and Trompette, 1980).

Geochronological data in the study area are still scarce and not yet integrated into a comprehensive model. A limited number of geochronological investigations with ages ranging from Archean to Neoproterozoic have been carried out in its nearest neighbourhoods, including: (i) a 2.1 ± 0.1 Ga U–Pb age of the reworked metasediments and orthogneisses basement from Touldoro (East of Ngaoundéré) (Toteu, Van Schmus, et al., 2001); (ii) a 2.1 ± 0.1 Ga U–Pb ages on hornblende–biotite gneisses of the Mbé region (Penaye et al., 1989); (iii) the $^{207}Pb/^{206}Pb$ ages on pyroxene–amphibole gneiss from Meiganga region (Ganwa et al., 2008) ranging from ~2.6 ± 0.1 Ga for inherited Archean core to ~1.7 ± 0.04 Ga for Palaeoproterozoic magmatic domain; (iv) the Th–U–Pb monazite ages on the Ngaoundéré biotite–muscovite granites and biotite–granite between 615 ± 27 and 575 ± 8 Ma (Tchameni et al., 2006) and (v) U–Pb zircon ages from Sassa-Mbersi ranging from 725 ± 12 Ma for the sedimentary protolith to 573 ± 2 Ma corresponding to emplacement of pegmatite dykes along dextral shear zones (Saha-Fouotsa et al., 2019).

In Tcholliré and Banyo regions, U–Pb and Sm–Nd dating of zircons and garnet-whole rock pairs yield ages ranging from Palaeoproterozoic to Neoproterozoic, considered as dating inheritances. Zircon overgrowths and recrystallised domains give U–Pb ages ranging between 604 ± 4 and 594 ± 8 Ma, interpreted as corresponding to HP granulite-facies metamorphism, in accordance with Sm–Nd garnet-whole rock ages. Sediments were deposited after 620 Ma from Palaeoproterozoic to Neoproterozoic protoliths (Bouyo Houketchang et al., 2009).

Palaeozoic events marking the post-tectonic granitoids from Adamawa-Yadé domain have been highlighted by Rb–Sr dating (Toteu, Michard, et al., 1986) and the discovery of Cambrian–Devonian detrital igneous zircons in conglomerates of the Tibati region. Whole-rock Rb–Sr dating carried out by Lasserre (1967) and Tempier et al. (1981) on the granitoids gave an age range of 531 ± 19 Ma to 558 ± 40 Ma; subsequently, Toteu, Michard, et al. (1986) obtained a Rb–Sr isochron age of 546 ± 9 Ma in the Godé massif, and U–Pb ages on Baddeleyite of the dolerites veins north of Ngaoundéré (542 ± 4 Ma on dolerites of Mbaoussi; 542 ± 4 Ma, 543 ± 5 Ma and 536 ± 6.4 Ma on those of Nomé).

3. Field descriptions

The study area includes two main lithologic units: volcanic and granitic rocks. Volcanic rocks outcrop as dome-shaped massifs or lava flows generally elongated in a preferential direction and occasionally as dykes intersecting granites. The lava flows are usually prismatic, massive, or vacuolar.

Granitoids consist of biotite- and biotite-amphibole-granites, locally banded or deformed and cropping out as massifs, metric boulders, slabs, or domes. The banded structure is often reinforced by migmatisation. Fine-grained rocks are mesocratic to melanocratic and generally outcrop either as injections within corridors delimited by quartzofeldspathic veins or as enclaves. Two local phases of deformation D_1 and D_2, are perceptible. The D_1 phase is marked by S_1 foliation dipping 30° toward NNE with a strike orientation of N100–125°E

(Figure 2a). This foliation is often straightened out and underlined by a lithologic banding materialised by dark ferromagnesian (amphibole ± biotite) layers alternating with clear quartz-feldspathic layers. The D_2 phase is represented by a mylonitic S_2 foliation striking N45–50°E and dipping 70NW to subvertical (Figure 2b,c), the boudinage (B_2) and the (L_2) stretching lineation. The S_2 results from the transposition of S_1 (Figure 2c), possibly due to dextral shear, resulting in the development of a new composite S_2/C_2 fabrics. The brittle deformation is represented by punch-through cracks, joints, and sub-meridian faults (Figure 2d). Dry joints are sub-vertical or parallel to the topographic surface, with a global N–S direction. Filled joints are basaltic dykes or pegmatitic to fine-grained veins (Figure 2d,e). Dextral strike-slip and ductile brittle faults are locally noticeable. The ductile brittle fault conveys the direction N45–50°E, 70°NW and is accompanied by numerous fractures oriented N135E–N150°E dipping 70–80°SW.

4. Methodology

4.1. *Samples collection and specimen preparation*

Fresh representative granitic rocks were collected in an area of about 50 km diameter at Ngaoundéré city vicinities in central-northeastern Cameroon (see Table 2 for their locations). Polished thin sections were prepared following standard procedures for petrographic observations and dating. Five representative samples were selected based on their petrography for X-ray fluorescence analyses and K–Ar dating in Mexico at the *Laboratorio Nacional de Geoqumica y Mineraloga (LANGEM), Instituto de Geologa, Universidad Nacional Autónoma de México (UNAM).*

4.2. *Analytical methods*

Bulk rock major elements were measured using a Rigaku Primus II X-ray fluorescence spectrometer calibrated with international reference materials. The rock samples were dried at 110 °C for 2 h before analyses. To prepare the glass tablet, 0.8 g of dry powder was mixed with 7.8 g of $Li_2B_4O_7$ and heated in a gas furnace to fusion to obtain a pearl. Loss on ignition (LOI) was determined with 1 g of dry sample powder calcined at 1000 °C for 1 h, and the mass loss was subsequently determined.

For K–Ar dating, the rock samples were chosen after petrographic observation, based on the presence of well-preserved biotite flakes. Samples were cut, glued with UV-cured epoxy, and polished with diamond paste to obtain standard thin polished sections of 27 × 46 × 0.03 mm. The slides were mounted within an ultrahigh vacuum chamber and prepared for the in-situ K–Ar system. The automatised analytical system described in detail by Solé (2014) and Solé (2021) is made of a noble gas mass spectrometer MAP 216 connected to a stainless steel ultra-high vacuum line. The line has two SAES GP-50 getters (one at 250 °C and the other at room temperature) to clean the gases evolved after ablating the sample. The line is also connected to an ultra-high vacuum chamber with a double window for transmitted light observation of the thin sections mounted inside. Light can be polarised to identify the crystals to be analysed. The ablation is done with an excimer ATL-RX laser with a wavelength of 193 µm, using a beam diameter of 50 or 70 µm, a repetition rate of 30–50 Hz, and 200 pulses. Fluence on samples was ~3 J cm^{-2}, and ablation pits were about 20 µm depth. During the ablation process, a small plasma is produced, whose light is sampled by an optical spectrometer to obtain the K concentration. The resultant gas, after cleaning, is equilibrated into the mass spectrometer for Ar measurement. The Supplemental Material section contains a detailed analytical protocol and additional sample's information. Supplement S1 includes petrographic microscope photographs of all analysed points in plane-polarised light and crossed Nicols. Readers can verify the ages of each point and their mineralogical/textural positions. It is important to highlight that this method has revealed that in micas from rocks subjected to deformation or metamorphism, a simple age gradient derived from diffusion theory does not explain the patterns well. The minerals in contact with the dated mica play a crucial role in fluid circulation and the ease of argon diffusion. Furthermore, age dispersions may vary based on the rock type and the preservation of the micas.

5. Results

5.1. *Descriptive petrography*

The studied rocks display a fine- to coarse-grained equigranular to heterogranular magmatic structure

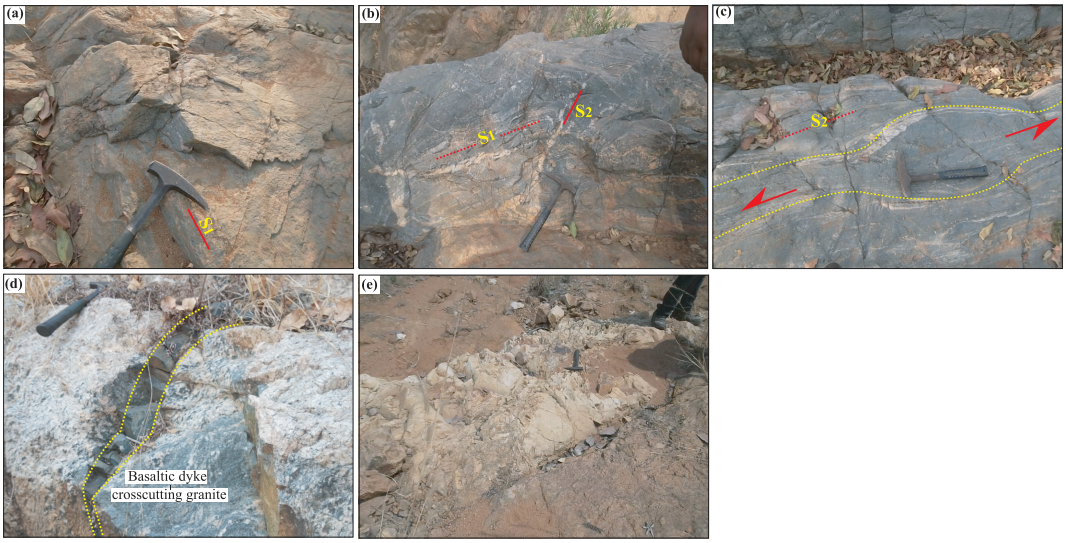

Figure 2. Some deformation markers of the basement rocks of the studied area. Ductile deformation (a–c) in deformed granites: (a) S_1 foliation on Maboro stream bed, (b) S_2 Foliation taking over the S_1 with the presence of alkaline feldspar relics revealing the magmatic origin of the protolith, (c) Sigmoid boudin B2 illustrating a dextral motion. Brittle deformation (d,e): (d) Filled joints illustrated by a basaltic dyke crosscutting granite, (e) Punch fractures observed in deformed granite.

at a microscopic scale (Figure 3a,b). The primary mineral phase includes quartz, alkali feldspar, plagioclase, amphibole, and biotite. The accessory phases consist of opaque minerals, sphene, apatite, and zircon. The secondary mineral phase consists of chlorite, epidote, and sericite crystallised at the expense of biotite, amphibole and alkali feldspars respectively. Quartz appears as anhedral medium to coarse recrystallised phenocrysts or interstitial fine grains. Plagioclase crystals exhibit typical twin lamellas and generally enclose Fe–Ti-oxides, biotite, amphibole, chlorite, or apatite, while fine crystals are usually included in alkali feldspars. Alkali feldspars consist of anhedral to subhedral microcline and orthoclase crystals, locally displaying cross-hatched and Carlsbad twins. The largest crystals (>1 mm) frequently show perthites and myrmekites. Amphibole appears as anhedral to subhedral brown to greenish pleochroic crystals (Figure 3c,d). Phenocrystals are poikilitic (biotite + apatite + Fe–Ti-oxides), often zoned, and frequently show corroded margins, whereas microcrystals are interstitial. Biotite crystals are brown or greenish, with a regular cleavage. Fine crystals are either included in alkali feldspars (Figure 3a) or interstitial, while phenocrysts commonly enclose apatite, zircon, and opaque minerals (Figure 3d). Opaque minerals generally appear as rounded, angular, or skeletal crystals, especially concentrated in the interstitial phase or included in primary minerals. Phenocrysts enclose zircon and apatite. Zircon is euhedral with a polygonal or cubic shape and is regularly included in biotite or opaque minerals. Apatite mostly crystallises either as interstitial acicular or hexagonal microcrystals or as anhedral or rounded crystals included within feldspars or biotite (Figure 3c,d–f). The more or less deformed character of the studied granitoids is sufficiently perceptible on certain minerals such as biotites displaying typical microstructures of deformation such as the elongation biotites flakes, the reduction of the grain size of the mica aggregates by the nucleation of new micas, and rarely mineral cracking or folding bands.

5.2. *Nomenclature and geochemical features*

The study granitoids have K_2O, Na_2O and Al_2O_3 contents ranging respectively between 2.8–6.3 wt%, 3.2–4.8 wt% and 13–16.2 wt%, and low Mg# (13.2–25) as presented in Table 1. They are potassic regarding

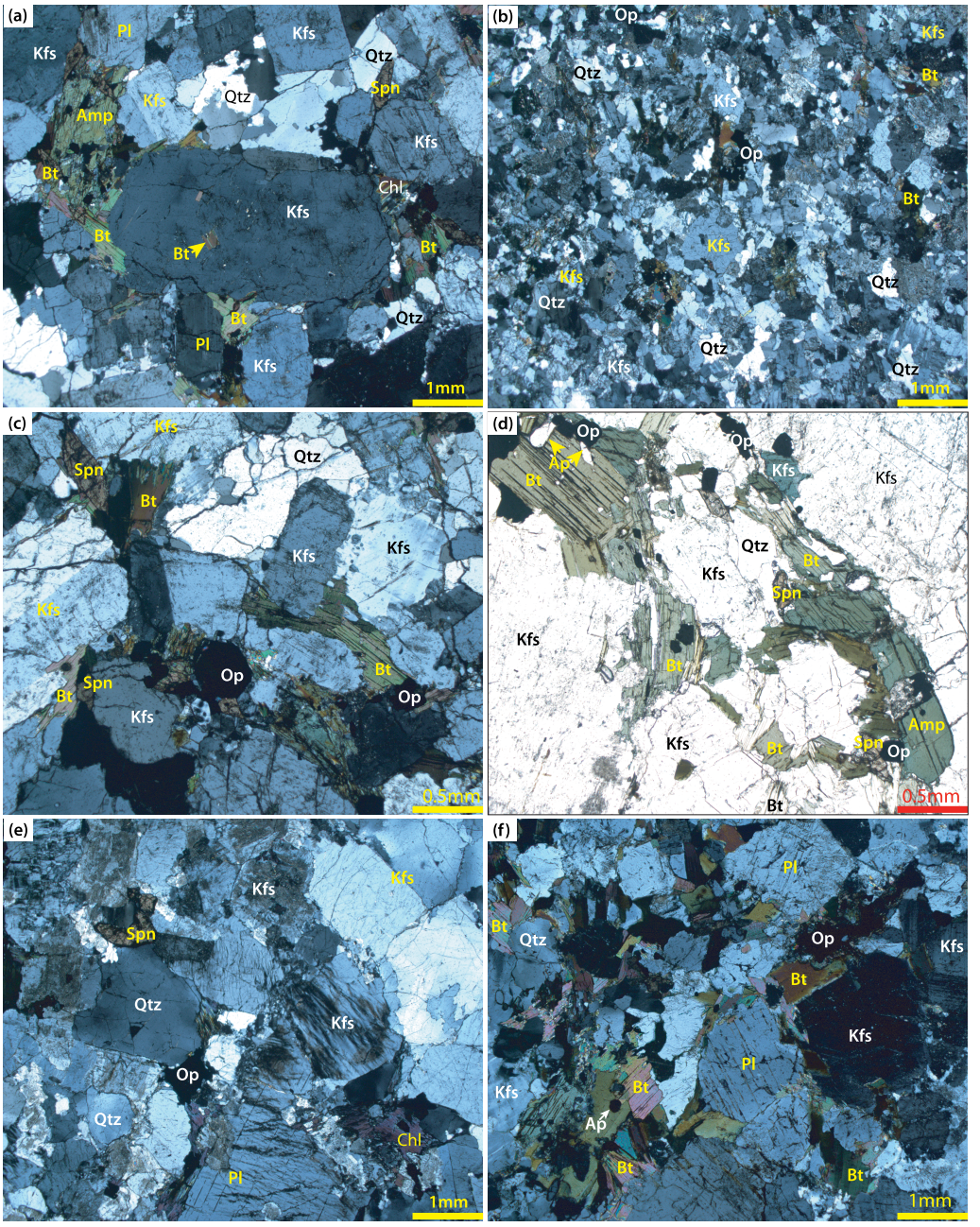

Figure 3. Representative photomicrographs for granitic rocks from Ngaoundéré. (a) Medium- to coarse-grained texture in Qz-monzonite BJM410 and inclusion of biotite microcrystal in alkali feldspar; (b) Fine-grained texture in granite BJM520; (c) Marks of deformation at microscopical scale in granite GAM521 revealed by bending of biotite cleavages and feldspars cracking; (d) Biotite flakes associated with euhedral sphene and hornblende including apatite and opaque minerals in Qz-monzonite BJM410; (e) Alkali feldspar exhibiting perthite in granite BIN089; (f) Zoned feldspar and biotite including apatite in Qz-monzonite BJM069. Mineral symbols are after Kretz (1983).

their Na_2O–K_2O values (<2) according to Le Bas et al. (1986). In the total alkali vs. silica (TAS) classification diagram of Middlemost (1994), they plot in the Qz-monzonite and granite fields (Figure 4A). Their normative composition is marked by (i) the presence of normative hypersthene (0.4–1.4 wt%) in all samples, and (ii) the occurrence of normative corundum, except in the Qz-monzonite sample (BJM 410) containing normative diopside (2.18 wt%). Three samples including two granites (BJM520 and BIN089) and Qz-monzonite BJM069 plot within the high-K to shoshonitic fields in the K_2O vs. SiO_2 diagram of Le Maître et al. (1989), one Bt-granite (GAM521) and one Qz-monzonite (BJM410) occupy the field of medium potassic rocks (Figure 4b). Considering their position in the diagram of Maniar and Piccoli (1989) and Chappell and White (1992) (Figure 4c), the study granitoids are calc–alkaline, of I-type, metaluminous to weakly peraluminous (A/CNK: 0.92–1.05; A/NK: 1.16–1.49). The slightly peraluminous granitoids belong to the ferroan series with Fe# (FeOt/FeOt + MgO) values ranging from 0.84 to 0.87 while metaluminous granitoids (Qz-monzonites) fit in the magnesian series (Figure 4d), with Fe# varying from 0.75 to 0.81 Regarding their high Na_2O contents (3.2–4.8 wt%) and their shoshonitic affinity (overall high K_2O/Na_2O ratio), the study granitoids likely display adakitic signature. Considering the low MgO (<3.0 wt%) and Mg# (mostly <45) of all the rocks displaying adakitic signature, they can be classified as low-Mg adakitic rocks. On the MgO and Mg# vs. SiO_2 discrimination diagrams, they respectively plot into the fields of high-silica adakite, and C-type adakites, likely derived from the melting of a thick lower crust (Figure 4e,f).

5.3. *Biotite K–Ar ages*

About 12 to 22 analyses on different biotite crystals have been done for each of the five selected samples. Overall, sixty-three (63) measurements were carried out but only forty (40) were retained for this study because analyses carried out on chloritised or altered biotites were not taken into account due to their erroneous values. The ages obtained using the in-situ K–Ar method are comparable to those from Ar–Ar via laser ablation, although with less precision. The advantage of this method is that it allows for age measurements in any polished sample without the need for irradiation. Individual laser ablation ages obtained in each dated samples range as follows: GAM521 (482–501 Ma), BJM410 (471–501 Ma) BJM069 (527–562 Ma), BIN089 (532–550 Ma) and BJM520 (527–595 Ma). Figure 5 shows the distribution of ages in the stratigraphic chart, and Table 2 displays the basic sample information. Dated samples display ages ranging from late Ediacaran (549 ± 19 Ma) to Early Ordovician (482 ± 6 Ma), covering 67 Myr of regional geological history and fitting together with the Pan-African orogenic phase in Cameroon, as discussed below (Table 2).

6. Discussion

6.1. *Laser K–Ar dating*

Geochronometers can be classified based on their diffusive blocking (closure) temperature. The U–Pb method applied to zircon and other trace minerals is typically restricted to high and ultrahigh-temperature events (>600 °C), such as the crystallisation of igneous rocks, migmatites, and the so-called high-grade metamorphism. However, medium and low-temperature events (<600 °C) that separate similar blocks from different geological evolutions, can sometimes be difficult or impossible to detect with the U–Pb method.

The laser K–Ar (or Ar–Ar) method is sensitive to temperatures below ~600 °C, deciphering medium to low-grade metamorphism, cooling, or hydrothermal circulation, contrary to the U–Pb method. The in-situ K–Ar method gives ages of different parts of crystals, like the Ar–Ar laser-probe method (Kelley et al., 1994; Mulch et al., 2002; Pickersgill et al., 2020), which can span a range of ages larger for one sample than the classical K–Ar, which shows only the weighted mean of all crystal ages measured. In this sense, the age range of each sample can be more comparable to the ages obtained with the Ar–Ar step heating approach. In-situ geochronology (e.g., K–Ar, Ar–Ar, Rb–Sr, U–Pb, Sm–Nd, Lu–Hf) applied to petrographic sections give spatial information not attainable by conventional techniques (bulk analyses, mineral separation). This added knowledge overcomes the fact that the precision of each analysis is lower due to the very small amount of sample analysed during laser ablation.

Table 1. Whole rock major elements chemical analyses of the analysed granitoids

Rock type	Sample	SiO_2	TiO_2	Al_2O_3	Fe_2O_3T	MnO	MgO	CaO	Na_2O	K_2O	P_2O_5	LOI	Total	A/NK	A/CNK	Mg#	Fe#
Qz-Monzonite	BJM410	62.93	0.76	16.22	5.84	0.10	1.95	3.90	4.81	2.78	0.33	0.38	100.00	1.49	0.90	25.01	0.75
	BJM069	67.58	0.55	14.97	4.27	0.05	1.12	2.08	3.71	5.03	0.23	0.42	100.00	1.30	0.98	20.83	0.79
Granite	BIN089	72.01	0.35	14.09	2.28	0.04	0.35	0.86	3.19	6.34	0.07	0.42	100.00	1.16	1.03	13.19	0.87
	BJM520	70.25	0.34	14.64	3.21	0.04	0.62	0.95	3.56	5.97	0.12	0.30	100.00	1.19	1.04	16.15	0.84
	GAM521	72.52	0.52	13.01	3.57	0.06	0.83	2.18	3.40	3.32	0.13	0.48	100.00	1.42	0.99	18.81	0.81

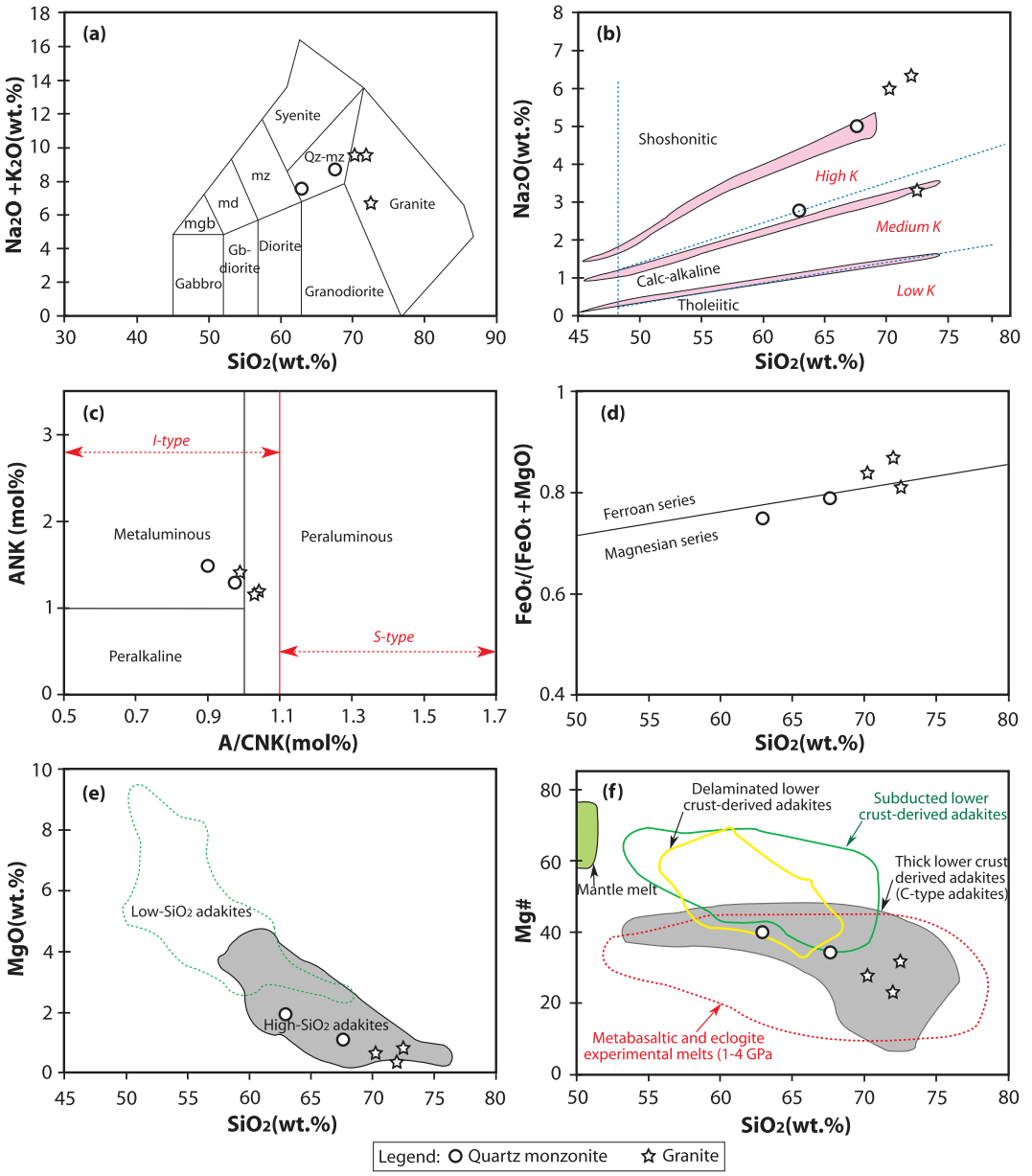

Figure 4. Nomenclature and chemical features of the dated rocks. (a) TAS diagram of Middlemost (1994); (b) K_2O vs. SiO_2 diagram illustrating the calc-alkaline and shoshonitic affinities of the analysed granitoids; the subdivisions are after Le Maître et al. (1989) and Rickwood (1989); (c) A/NK [molar $Al_2O_3/(Na_2O + K_2O)$] vs. A/CNK [molar $Al_2O_3/(CaO + Na_2O + K_2O)$] diagram after Maniar and Piccoli (1989). The borderline between I-type and S-type granites is after Chappell and White (1992); (d) $FeO_T/(FeO_T + MgO)$ vs. SiO_2 diagram; (e) MgO vs. SiO_2 diagram showing the high-silica adakite affinity of the dated granitoids. The respective fields in the diagram are derived from Martin et al. (2005); (f) plots of Mg number vs. SiO_2. Fields of delaminated lower crust-derived adakitic rocks, subducted oceanic crust-derived adakites and thick lower crust-derived adakitic rocks were built by Wang et al. (2005).

Table 2. Biotite K–Ar dating results of granitic rocks from the study area

Rock type	Qz-monzonite		Granite		
Sample code	BJM410	BJM069	BIN089	BJM520	GAM521
Location	07°37′17.3″N 13°46′05.5″E	07°33′51.3″N 13°54′49.3″E	07°37′35.5″N 13°55′03.1″E	07°38′34.9″N 14°16′10.4″E	07°34′20.4″N 13°40′43.3″E
Altitude (m)	1320	867	889	789	1138
Mineralogical assemblage	Qz + Kfs + Pl + Bt + Spn + Amp + Zrn + Ep + Ox	Qz + Kfs + Pl + Bt + Spn	Qz + Kfs (Mc) + Pl + Bt + Spn + Ox	Qz + Kfs (Mc) + Pl + Bt + Amp +Spn + Zrn + Ep + Ox	Qz + Kfs + Bt + Amp + Pl + Spn + Zrn + Ox
Individual laser ablation age (Ma)	483	556	532	543	501
	496	543	524	529	484
	482	562	518	543	500
	501	560	522	546	482
	498	530	522	527	
	471	540	505	593	
	490	527	524	575	
	488	541	522	563	
	482		527		
	498		517		
Average age (Ma)	495 ± 10	521 ± 17	538 ± 18	549 ± 19	482 ± 6

For mineral symbols, Qz = quartz; Kfs = Potassic feldspar, Pl = Plagioclase; Bt = biotite; Spn = sphene; Amp = Amphibole; Zrn = zircon; Ep = epidote; Ox = oxide; Mc = microcline.

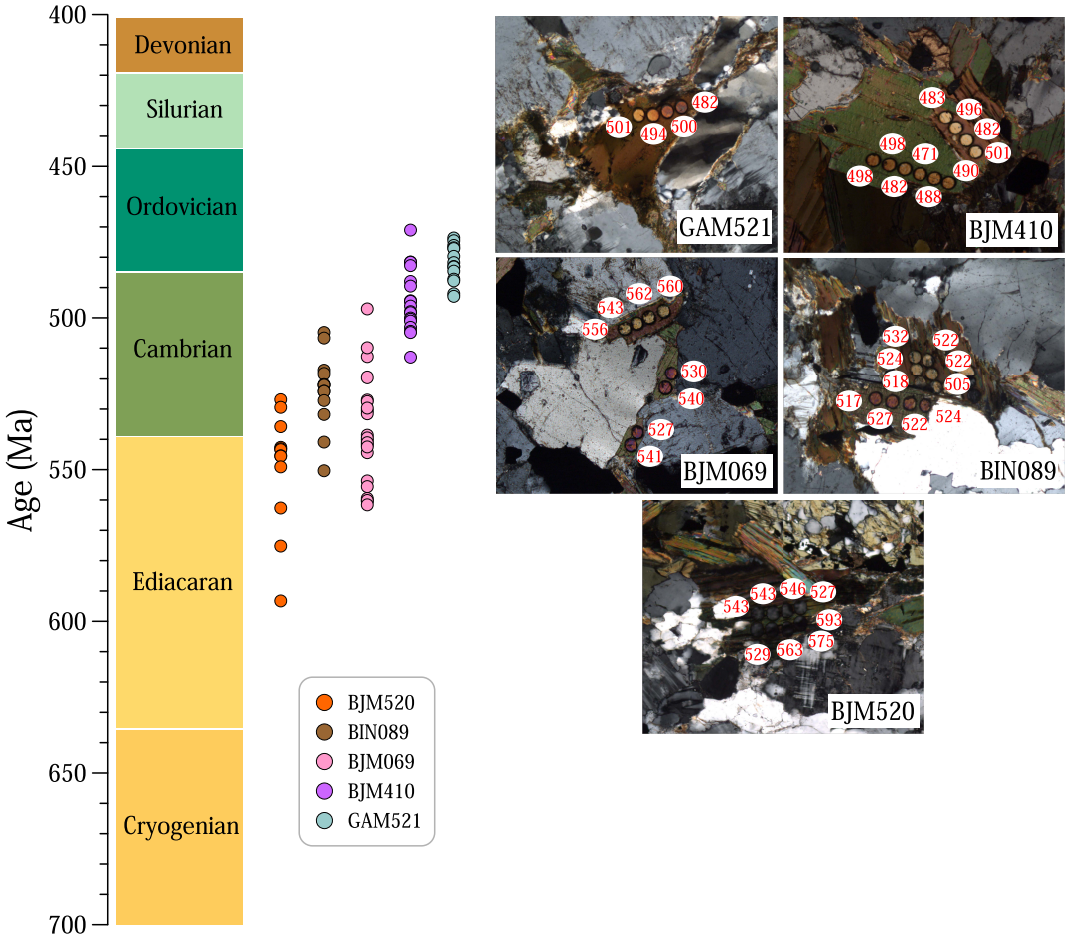

Figure 5. In-situ K–Ar ages on biotites obtained in standard petrographic thin sections of five granitic rocks near Ngaoundéré, Cameroon. Each point corresponds to an individual laser ablation age. A minimum of 12 analyses per sample have been obtained, with a total of 40 ages (see Table 2). The range of ages for each sample is mainly influenced by later metamorphic events. At the right are photographs of some dated biotites, showing laser ablation craters and their ages in Ma.

These medium-temperature geochronometers could discriminate rocks that experienced a different geological history even if the protoliths were the same or the samples were spatially grouped by tectonic activity. Moreover, the direct dating of thin sections allows checking the petrology of samples and selecting the appropriate minerals to be dated, producing a strong test on ages. If better precision and further interpretative control are needed, the Ar–Ar method will be more appropriate, assuming the additional analytical effort. Other low-temperature thermochronometers like fission tracks or U–Th–He will complement the interpretation of the tectonic history of Precambrian samples in cratonic regions worldwide. Nevertheless, the K–Ar (or Ar–Ar) methodology preserves, in general, a more detailed record of cooling or overprinting. These ages may indicate the time since the mineral (re)crystallisation. Still, because most igneous and metamorphic rocks can form at moderate to high temperatures, most dates indicate the length of time since the material dropped below some critical temperature known as closure temperature at which diffusion of argon out of the sample became negligible (e.g., Philpotts and Ague, 2010). The K–Ar dating method differs from other common methods by involving a decay

product that is an inert gas, not affected by initial isotopic ratios, as is the Rb–Sr method. Even at moderately low temperatures, this gas is a fugitive component (i.e., has very low solubility) and is typically not incorporated in minerals (e.g., ibid.).

6.2. *Geodynamic significance and implications on the Post-Pan-African evolution*

Two major facts are remarkable with regard to the Post-orogenic ages presented in Table 3: (1) Few Paleozoic igneous events have been reported in the Adamawa-Yadé domain; and (2) the K–Ar ages presented in this study (549 ± 19 to 482 ± 6 Ma) are among the youngest obtained so far in the CAPFB. As much as these Paleozoic ages linked to the Pan-African orogeny have been interpreted either as emplacement ages particularly for the granitoids from northern Cameroon (Lasserre, 1967; Tempier et al., 1981; Toteu, Michard, et al., 1986), or erroneously ascribed to the extension of post-collisional metamorphism and magmatism related to the late collision phases between the Saharan metacraton, the São Francisco-Congo and West African cratons (despite the absence of a regional Cambrian metamorphic event recorded in the CAPFB) by Kanouo et al. (2021), their magmatic source remains unidentified.

The age range obtained in the present work overlaps the period of Late Cambrian post-orogenic magmatism recorded in Kékem (Lemdjou et al., 2022) (see Table 3), and is consistent not only with the maximum emplacement age for post-tectonic granitoids in northern Cameroon (554.3 ± 5.7 Ma; Toteu, De Wit, et al. (2022), but also with the Rb–Sr ages (550–500 Ma) recorded in post-tectonic alkaline granites emplaced subsequent to the uplift of the Pan-African fold belt (Toteu, Van Schmus, et al., 2001). However, assuming that: (1) Post-tectonic granitoids in the Adamawa-Yadé domain were emplaced between 604 ± 8 and 544 ± 16 Ma (Toteu, De Wit, et al., 2022), (2) most of plutonic intrusions throughout Nigeria, Cameroon, and Aïr were emplaced between 645 and 580 Ma and (3) a large proportion of them intruded at about 580 Ma (Liégeois et al., 1994; Ekwueme and Kröner, 1998; Ferré et al., 1998), the new ages range presented in this work is too young to be considered as the crystallisation age of magmas. They likely correspond to the late stages of the Pan-African Orogeny. Therefore, the dated granitoids are likely the fingerprints of late- to post-orogenic events in the area. They have intruded the early Pan-African metamorphic units in the late stages of the Brasiliano/Pan-African orogenic evolution later to the 640–580 Ma compressional tectonic regime of the CAPFB.

The new laser biotite K–Ar ages may correspond to metamorphism or deformation subsequent to the emplacement of the dated rocks. The Late Ediacaran ages might provide insight into the timing of late Adamawa-Yadé kinematics and probably the uplift and cooling of the CAPFB. Otherwise, the Adamawa uplift and cooling of the CAPFB are post-metamorphic and post-tectonic events that mark the end of convergence and the beginning of crustal extensional. Thus, Cambrian intrusions associated with these events mark the transition between convergence and divergence in CAPFB.

As presented in Table 3, all the Cambrian to early Ordovician ages, are mostly linked to Post-Pan-African events in Cameroon. Moreover, it is noteworthy that in Cameroon, the earliest Pan-African molasses (generally defined as post-collision detrital sediments) in CAPFB to date are the Mangbai-type through (Béa et al., 1990), the syn-trough deposits approximated Rb–Sr age of interleaves volcanic is ca 585 Ma (Montes-Lauer et al., 1997). Therefore, in absence of additional mineralogical and structural/tectonic data, the new K–Ar ages (549 ± 19–482 ± 6 Ma) here presented, can more likely be ascribed to the late stage of the Pan-African orogeny in CAPFB as it is the case for the Cambrian–Ordovician ages of the Brazilian Belt or NE–Nigeria, than to an independent event such as rifting or strike-slip. Rifting and/or strike-slip in Cambrian–Ordovician times were most likely related to further isostatic evolution of CAPFB, in response to the equilibration of the Pan-African thickened crust during nappes stacking.

The entirely Ediacaran age (558–630 Ma) of the late Pan-African plutonism phase of the Eastern Adamawa region including our study area as stated by Bernard et al. (2019) and Delor et al. (2021) is questioned in the present work, because the new ages obtained evidence that this phase might be longer and undoubtedly extends until the end of the Cambrian. A relevant fact on similar ages in nearby blocks and domains must be mentioned first. Although some

Table 3. Post-Pan-African ages of some localities from the Cameroon

Locality	Age (Ma)	Rock type	Method	Reference
Tibati-Banyo	~598 to ~568	Gneiss	U–Pb zircon	Bernard et al. (2019)
Djerem-Mbéré basin	540–371	Conglomerates	U–Pb zircon	Bernard et al. (2019)
Kékem	576 ± 4	Alkaline gabbro	LA–ICP–MS U–Pb	Kwékam et al. (2013)
Bouar	566.4 ± 7.0	Granite	U–Pb zircon	Toteu, De Wit, et al. (2022)
Béa	562.7 ± 2.1	Amphibolite	U–Pb zircon	Toteu, De Wit, et al. (2022)
Rocher de Loup	519± 19	Nepheline syenite	U–Pb zircon	Nsifa Nkonguin et al. (2013)
Guider	593 ± 4	Syenite	U–Pb zircon	Dawaï et al. (2013)
Dschang	421.3 ± 3.5	Basalt	$^{40}Ar/^{39}Ar$	Tchouankoué et al. (2014)
Maham	404.2 ± 3.2–417 ± 8	Basalt	K/Ar and$^{40}Ar/^{39}Ar$	Tchouankoué et al. (2014)
Kékem	486 ± 15–497 ± 14	Gabbro	U–Pb zircon	Lemdjou et al. (2022)
Godé	546 ± 9	Granite	Rb/Sr WR isochron	Toteu, Michard, et al. (1986)
Balché	440	rhyolite	Whole rock K/Ar	In Lasserre et al. (1977)
Mangbai basin	373± 10–425 ± 12	Volcanic rocks	Whole rock K/Ar	Béa et al. (1990)
Mamfe	~536–~449	Granite and gneiss	U–Pb zircon	Kanouo et al. (2021)

retrogression processes may be recorded, no regional metamorphism has been signalled during the uplift. The new ages correspond to K–Ar on biotite of grain sizes from ~1 mm to ~0.5 mm, so if we apply the theory of diffusion to this mineral using the experimental data, the temperature of closure (assuming only Fickian diffusion controlled by temperature) is 350–400 °C. Most of the geochronology of Cameroon, particularly Precambrian terranes, has been done with the U–Pb geochronometer on zircon, which has a very high temperature of closure, magmatic in general. For age analysis, a density diagram has been created for each sample, assuming a 2% variation for each Gaussian curve of each age. Uncertainty in K–Ar ages has been calculated using standard methods that rely on normal error propagation. Precision is derived from analytical argon measurements taken with the mass spectrometer, and potassium from measurements taken with the optical spectrometer. Accuracy is established through the analysis of internal standards. The set of curves, which has been fitted with one or more functions to determine the centre and standard deviation, is displayed in Figure 6. BIN089 is unimodal with a centre at 523 ± 17 Ma. The dispersion appears to be associated with analytical uncertainty and the cooling of the sample below the biotite closure temperature, nominally between 300 °C and 400 °C. BJM069 shows a main peak at 543 ± 20 Ma and a secondary one at 515 ± 20 Ma. We consider the first peak to represent the sample age and the second to indicate a potential "reset" of some analysed points. BJM410 can be regarded as having an age of 495 ± 17 Ma, with a slight curve deformation that could be divided into two at 492 ± 17 and 501 ± 12 Ma. The difference is not significant, and the first age is accepted as valid. BJM520 presents a main peak at 541 ± 16 Ma, accompanied by a small adjacent peak at 581 ± 20 Ma. The fact that the secondary peak is older suggests an excess of argon in some of the analysed micas. Thus, we consider the first age to be the best estimate. GAM521 has a single, well-defined peak at 482 ± 13 Ma. Therefore, the oldest spot obtained on the Amph–Bt-granite BJM520 (549 ± 19 Ma) could be considered to be closest to the intrusion and the lower ages reported in this work, although similar to some early Palaeozoic late Pan-African intrusions cited above, can be interpreted as the final epoch of cooling of the analysed rocks or a last disturbance of the K–Ar geochronometer on biotite. Therefore, this range (from 538 ± 18 Ma to 482 ± 6 Ma) likely corresponds to either cooling by uplift fluid movements due to tectonic events or kinematic disturbances rather than a long period of intrusions.

6.3. *Comparison and correlation with the adjacent Brazilian Belt*

The tectonic evolution of both the CAPFB and the Brazilian fold belt is characterised by three main tectonic events involving collision, post-collision, and crustal extension, suggesting that both formed a single belt before they drifted in Mesozoic, although the sequential limits of the above events are still controversial (Ngako and Njonfang, 2011; Toteu, De Wit, et al., 2022). The correlation of the CAPFB with the Brasiliano fold belt (Figure 7) has allowed highlighting some similarities between the two belts both in terms of the orogenic cycle and their tectonic evolution (De Wit et al., 2008). This is the reason why we propose to make a summary comparison of the K–Ar ages obtained in the present work with some published data of the post-collision episodes of the east coast of Brazil, although the Adamawa-Yadé domain does not seem to extend overseas. The Cambro-Ordovician post-collisional phase of the Brasilano fold belt is characterised by intense magmatic activity clearly visible both in the SE and NE of Brazil and even in the central zone (Castro, Basei, et al., 2009; Castro, Ganade de Araujo, et al., 2012; Teixeira, 2005) and Rio Grande do Norte (Nascimento et al., 2015).

In SE-Brazil, Cambrian to early Ordovician post-collisional magmatism has been dated in Araçuai-Ribeira belt precisely in the region of Espirito Santo. The U–Pb ages obtained on zircon, monazite and titanite range from 525 ± 3 Ma to 480.7 ± 6.1 Ma (Mendes et al., 2005; Valeriano et al., 2011; de Campos, Mendes, et al., 2004; de Campos, De Medeiros, et al., 2016). These ages were associated with the third phase of anatexis (de Campos, Mendes, et al., 2004) and correspond to the emplacement and crystallisation ages. During this post-collisional Cambro-Ordovician phase, two distinct magmatic events were highlighted in this SE-Brazilian region: (i) an earlier of Cambrian age (~ca.512 Ma) post-dating the end of the foremost collisional phase, then (ii) the late one of Ordovician age (~at ca.486 Ma) post-dating the end of the second collisional episode. In the Parana

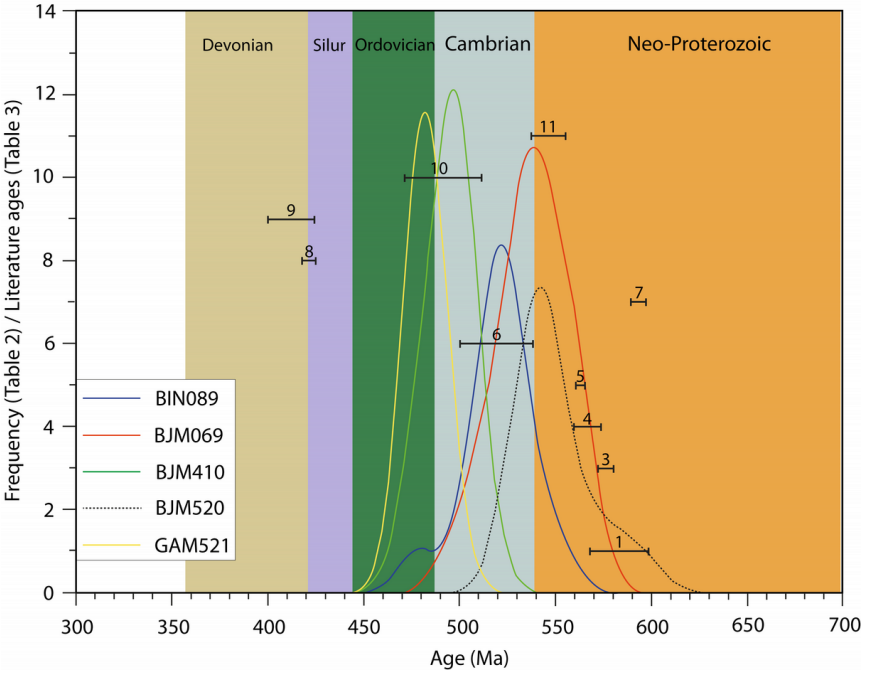

Figure 6. Density diagram of dated samples individual K–Ar ages. The numbered horizontal bars indicate the ages (including the margin of error) presented in Table 3, listed in sequential order, starting from the first line of the table. Some large age ranges from Table 3 have not been included.

and Parnaiba basins, the post-collision Ordovician magmatism was emplaced in an extensive regime and associated with the Trans-Brasiliano Shear Zone (Brito Neves et al., 2014; Heilbron et al., 2018).

In the NE Brazil, the Palaezoic magmatism has been identified in the northernmost continuation of the Trans-Saharan Belt known as the Brasilian Seridó belt (520 ± 3.0–518 ± 1.8 Ma; $^{40}Ar/^{39}Ar$ ages; Araújo et al. (2005)), and widely distributed in the Borborema Province (BP) particularly in the Piancó-Alto Brigida domain (540 ± 5 Ma; U–Pb apatite dating; Dhuime et al. (2003)), the Prata Complex (534 ± 3 Ma–533 ± 4 Ma; U–Pb zircon SHRIMP; Hollanda et al. (2010)), and numerous plutons including the Serra do Velho Zuza (538 ± 23 Ma; U–Pb zircon TIMS), Serra do Pereiro (543 ± 7 Ma; U–Pb zircon TIMS) (Guimarães, Silva Filho, Almeida, et al., 2004), Marinho Pluton (550 ± 3 Ma–527 ± 6 Ma; U–Pb zircon SHRIMP; Guimarães, Silva Filho, Lima, et al. (2012)), and Queimadas (550 ± 6 Ma; U–Pb Zircon SHRIMP; Almeida et al. (2002)) In the Seridó belt it was ascribed to the likely post-peak metamorphism age associated with gold mineralisation (Araújo et al., 2005) while in the BP which is generally considered as an extension of the CAPFB in pre-drift reconstructions of the Atlantic Ocean (Guimarães, da Silva Filho, et al., 2009; Oliveira et al., 2006; Toteu, Van Schmus, et al., 2001) (see Figure 7), the Cambrian ages were interpreted as cooling age following regional metamorphism associated with granitic emplacement at ca. 580 Ma in Piancó-Alto Brígida belt (Dhuime et al., 2003). Thus, despite slight shifts, similarities emerge between the K–Ar ages obtained in the present work and those of the post-collision episodes from eastern coast of Brasilian belt.

7. Conclusions

This study reports new in-situ K–Ar geochronological data on thin sections of five granitic rocks from Eastern Ngaoundéré in Cameroon. The analysed calk-alkaline I-type plutonic rocks consist of Qz-monzonite and granite. Their dating provided significant ages ranging from late Ediacaran (549 ± 19 Ma) to Early Ordovician (482 ± 6 Ma). They are among the youngest ages published in the

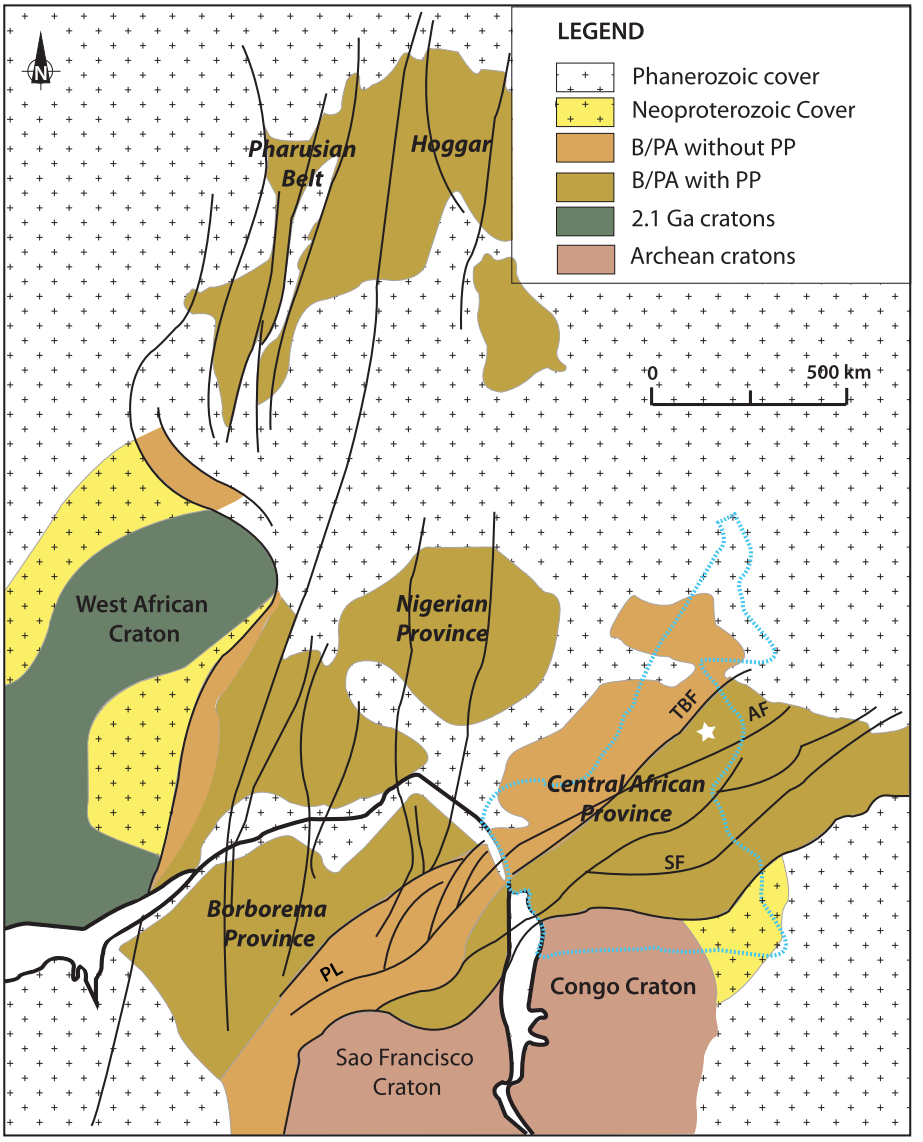

Figure 7. Generalised geological map of NE-Brazil and West-central Africa in a Gondwana (pre-drift) configuration (modified from Toteu, Van Schmus, et al., 2001). The blue dashed outline indicates the boundary of Cameroon. TBF = Tcholliré-Banyo Fault (in Cameroon); SF = Sanaga Fault (in Cameroon); PL = Pernambuco Lineament (in Brazil); AF = Adamawa Fault (in Cameroon). The white star approximately locates the study area. "B/PA with PP" states to regions of Brazilian-Pan-African belt with large amounts of reworked Palaeoproterozoic basement; "B/PA without PP" refers to regions of Brazilian-Pan-African belt in which Palaeoproterozoic basement is absent or poorly represented as small isolated blocks.

Pan-African Adamawa-Yadé domain. These new ages obtained mark the extensional regime in the earliest stages of the Adamawa uplift between the late Ediacaran to Early Ordovician as well as the end of the CAPFB orogen, implying no later disturbance of the argon system in biotite after ~480 Ma.

Declaration of interests

The authors do not work for, advise, own shares in, or receive funds from any organization that could benefit from this article, and have declared no affiliations other than their research organizations.

Acknowledgments

The authors deeply thank Teresa Pi Puig and Rufino Lozano of the LANGEM (UNAM, Mexico) for the X-ray diffraction and whole rock analyses presented in this paper, then Professor Alembert Ganwa (Ngaoundéré University) for constructive discussions. We also thank Professor Rigobert Tchameni and Michel Villeneuve for their significant and constructive comments, and the editorial assistance from Michel Faure.

Supplementary data

Supporting information for this article is available on the journal's website under https://doi.org/10.5802/crgeos.289 or from the author.

References

Almeida, C. N., I. P. Guimarães and A. F. Silva Filho, "A-type post-collisional granites in the Borborema Province-NE Brazil: The Queimadas Pluton", *Gondwana Res.* **5** (2002), pp. 667–681.

Araújo, M. N. C., P. M. Vasconcelos, F. C. Alves da Silva, E. F. Jardim de Sá and J. M. Sá, "^{40}Ar/^{39}Ar geochronology of gold mineralization in Brasiliano strike-slip shear zones in the Borborema province, NE Brazil", *J. Afr. Earth Sci.* **19** (2005), pp. 445–460.

Béa, A., J. J. Cochemé, R. Trompette, P. Affaton, D. Soba and J. Sougy, "Grabens d'âge Paléozoïque inférieur et volcanisme tholéiitique associé dans la région de Garoua, Nord Cameroun", *J. Afr. Earth Sci.* **10** (1990), pp. 657–667.

Bernard, J., O. Blein, R. Couëffe, et al., *1:200.000-scale geological map of Cameroon-Sheet Ngaoundere (NB–33–XX)*, 2019. Explanatory Notes, 110pp.

Bessoles, B. and R. Trompette, "La chaîne pan-africaine "zone mobile d'Afrique centrale (partie sud) et zone mobile soudanaise"", *Mem. BRGM* **92** (1980), p. 396.

Bouyo Houketchang, M., S. F. Toteu, E. Deloule, J. Penaye and W. R. Van Schmus, "U–Pb and Sm–Nd dating of high-pressure granulites from Tcholliré and Banyo regions: Evidence for a Pan-African granulite facies metamorphism in north central Cameroon", *J. Afr. Earth Sci.* **54** (2009), pp. 144–154.

Brito Neves, B. B., A. R. Fuck and M. M. Pimentel, "The Brasiliano collage in South America: a review", *Braz. J. Geol.* **44** (2014), pp. 493–518.

Castaing, C., J. L. Feybesse, D. Thieblemont, C. Triboulet and P. Chevremont, "Paleogeographical reconstructions of the Pan-African/Brasiliano orogen: closure of an oceanic domain or intracontinental convergence between major blocks", *Precamb. Res.* **69** (1994), pp. 327–344.

Castro, N. A., M. A. S. Basei, L. S. Osako, A. P. Nutman and L. Dunyi, "U–Pb SHRIMP and ID–TIMS ages of Ordovician anorogenic granitoid magmatism at Taperuaba region, Ceará Central Tectonic Domain, Northeast Brazil", in *Simpósio 45 anos de Geocronologia no Brasil. Boletim de Resumos Expandidos*, 2009, pp. 224–226.

Castro, N. A., C. E. Ganade de Araujo, M. A.S. Basei, L. S. Osako, A. A. Nutman and D. Liu, "Ordovician A-type granitoid magmatism on the Ceará Central Domain, Borborema Province, NE-Brazil", *J. South Am. Earth Sci.* **36** (2012), pp. 18–31.

Chappell, B. W. and A. J. R. White, "I- and S-type granites in the Lachlan fold belt", *Trans. Roy. Soc. Edinb. Earth Sci.* **83** (1992), pp. 1–26.

Coulon, C., P. Vidal, C. Dupuy, P. Boudin, M. Popoff, H. Maluski and D. Hermille, "The Mesozoic to early Cenozoic magmatism of the Benue Through (Nigeria): geochemical evidence for the involvement of the St", *Helena Plume. J. Petrol.* **3** (1996), pp. 1341–1358.

Dawaï, D., J.-L. Bouchez, J.-L. Paquette and R. Tchameni, "The Pan-African quartz-syenite of Guider (North-Cameroon): Magnetic fabric and U–Pb dating of a late-orogenic emplacement", *Precambr. Res.* **236** (2013), pp. 132–144.

de Campos, C. P., S. R. De Medeiros, J. C. Mendes, A. C. Pedrosa-Soares, I. Dussin, I. P. Ludka and E. L. Dantas, "Cambro-Ordovician magmatism in the Araçuaí Belt (SE Brazil): Snapshots from a post-collisional event", *J. S. Am. Earth Sci.* **68** (2016), pp. 248–268.

de Campos, C. P., J. C. Mendes, I. P. Ludka, S. R. De Medeiros, J. Costa-de-Moura and C. M. Wallfass, "A review of the Brasiliano magmatism in southern Espírito Santo, Brazil, with emphasis on post-collisional magmatism", *J. Virtual Explor.* **17** (2004), article no. 1. Electronic Edition. ISSN 1441-8142.

De Wit, M. J., J. Stankiewicz and C. Reeves, "Restoring Pan-African–Brasiliano connections: more Gondwana control, less Trans-Atlantic corruption", in *West Gondwana: Pre-Cenozoic Correlations Across the South Atlantic Region* (Pankhurst, R. J., R. A. J. Trouw, B. B. de Brito Neves and M. J. De Wit, eds.), Geological Society, London, Special Publications, Geological Society of London, 2008, pp. 399–412.

Delor, C., J. Bernard, R. D. Tucker, et al., *1:1000000-scale geological map of Cameroon*, 2nd edition, Ministry of Mines, Industry and Technological Development: Republic of Cameroon, 2021.

Dhuime, B., D. Bosch, O. Bruguier, R. Caby and C. Archanjo, "An Early-Cambrian U–Pb apatite cooling age for the high-temperature regional metamorphism in the Piancó area, Borborema Province (NE Brazil): initial conclusions", *C. R. Géosci.* **335** (2003), pp. 1081–1089.

Djerossem, F., A. Zeh, M. Isseini, O. Vanderhaeghe, J. Berger and J. Ganne, "U–Pb–Hf isotopic systematics of zircons from granites and metasediments of southern Ouaddaï (Chad), implications for crustal evolution and provenance in the Central Africa Orogenic Belt", *Precambr. Res.* **361** (2021), article no. 106233.

Ekwueme, B. N. and A. Kröner, "Single zircon evaporation ages from the Oban Massif, southeastern Nigeria", *J. Afr. Earth Sci.* **26** (1998), pp. 195–205.

Ferré, E. C., R. Caby, J. J. Peucat, R. Capdevila and P. Monié, "Pan-African, post-collisional, ferro-potassic granite and quartz-monzonite plutons of Eastern Nigeria", *Lithos* **45** (1998), pp. 255–279.

Ganwa, A. A., W. Frisch, W. Siebel, G. E. Ekodeck, C. K. Shang and V. Ngako, "Archean inheritances in the pyroxene-amphibole-bearing gneiss of the Méiganga area (Central North Cameroon): Geochemical and $^{207}Pb/^{206}Pb$ age imprints", *C. R. Géosci.* **340** (2008), pp. 211–222.

Guimarães, I. P., A. F. da Silva Filho, B. D. de Araujo, C. N. de Almeida and E. Dantas, "Trans-alkaline magmatism in the Serrinha-Pedro Velho Complex, Borborema Province, NE Brazil and its correlations with the magmatism in eastern Nigeria", *Gondwana Res.* **15** (2009), no. 1, pp. 98–110.

Guimarães, I. P., A. F. Silva Filho, C. N. Almeida, W. R. Van Schmus, J. M. M. Araújo, S. C. Melo and E. B. Melo, "Brasiliano (Pan-African) granitic magmatism in the Pajeú–Paraíba Belt, Northeast Brazil: an isotopic and geochronological approach", *Precambr. Res.* **135** (2004), pp. 23–53.

Guimarães, I. P., A. F. Silva Filho, J. V. Lima, D. J. S. Farias, J. V. A. Amorim and F. M. J. V. Silva, "Geocronologia U–Pb e Caracterizacão Geoquímica Dos Granitoides Do Pluton Marinho, Província Borborema", in *Proceedings of the 46° Congresso Brasileiro de Geologia Anais Proceedings, Santos, Brazil*, 2012.

Guiraud, R. and J. C. Maurin, "Le rifting en Afrique au Crétacé inférieur : synthèse structurale mise en évidence de deux étapes dans la genèse des bassins, relations avec les ouvertures océaniques péri-africaines", *Bull. Soc. Geol. France* **162** (1991), pp. 811–823.

Heilbron, M., E. Guedes, M. Mane, et al., "Geochemical and temporal provinciality of the magmatism of the eastern Parnaíba Basin, NE Brazil", in *Cratonic Basin Formation: A Case Study of the Parnaíba Basin of Brazil* (Daly, M. C., R. A. Fuck, J. Julià, D. I. M. Macdonald and A. B. Watts, eds.), Geological Society, London, Special Publications, Geological Society of London, 2018.

Hollanda, M. H. B. M., C. J. Archanjo, L. C. Souza, R. Armstrong and P. M. Vasconcelos, "Cambrian mafic to felsic magmatism and its connections with transcurrent shear zones of the Borborema Province (NE Brazil): implications for the late assembly of the West Gondwana", *Precambr. Res.* **178** (2010), pp. 1–14.

Itiga, Z., J. M. Bardintzeff, P. Wotchoko, P. Wandji and H. Bellon, "Tchabal Gangdaba massif in the Cameroon volcanic line: a bimodal association", *Arab. J. Geosci.* **7** (2014), no. 11, pp. 4641–4664.

Kanouo, S. N., R. D. Lentz, K. Zaw, C. Makoundi, A. A. E. Basua, F. R. Yongué and E. Njonfang, "New insights into pre- to post-Ediacaran zircon fingerprinting of the Mamfe Pan-African basement, SW Cameroon: a possible link with rocks in SE Nigeria and the Borborema Province of NE Brazil", *Minerals* **11** (2021), no. 943, pp. 1–32.

Kelley, S. P., N. O. Arnaud and S. P. Turner, "High spatial resolution $^{40}Ar/^{39}Ar$ investigations using an ultra-violet laser probe extraction technique: Geochim", *Cosmochim. Acta* **58** (1994), pp. 3519–3525.

Kretz, R., "Symbols for rock-forming minerals", *Am. Min.* **68** (1983), pp. 277–279.

Kwékam, M., P. Affaton, O. Bruguier, J. P. Liégeois, G. Harmann and E. Njonfang, "The Pan-African Kékem gabbro-norite (West-Cameroon), U–Pb zircon age, geochemistry and Sr–Nd isotopes: geodynamic implication for the evolution of the central African fold belt", *J. Afr. Earth Sci.* **84** (2013), pp. 70–88.

Lasserre, M., *Carte géologique de reconnaissance de la République du Cameroun (Echelle 1/500000)*, 1961. Feuille Ngaoundéré–E. NB 33 N °E43. Dir. Mines Geol. Cameroun.

Lasserre, M., "Données géochronologiques nouvelles acquises au 1er Janvier par la méthode au Strontium appliquée à l'étude aux formations cristallines et cristallophylliennes du Cameroun", *Ann. Fac. Sci. Univ. Clermont-Ferrand* **36** (1967), no. 16, pp. 109–144.

Lasserre, M., J. C. Baubron and J. M. Cantagrel, "Existence d'une couverture non plissée d'âge paléozoïque inférieur au sein de la zone mobile de l'Afrique centrale: âge K/Ar des formations de type Mangbai", *C. R. Acad. Sci., Paris, D* **284** (1977), pp. 2667–2670.

Le Bas, M., R. Le Maitre, A. Streckeisen and B. Zanettin, "A chemical classification of volcanic rocks based on the total alkali-silica diagram", *J. Petrol.* **27** (1986), no. 3, pp. 745–750.

Le Maître, R. W., P. Bateman, A. Dubek, et al., "A classification of igneous rocks and glossary of terms", in *Recommendations Int. Union Geol. Sci. Sub commission on the Systematic of Igneous Rocks*, Blackwell: Oxford, 1989.

Lemdjou, Y. B., T. D. P. I. Tchaptchet, H. Li, S. A. Whattam, S. L. Tamehe, S. M. Elatikpo and N. Madayipu, "Cambrian mafic magmatism in the Kékem area, NW edge of the Adamawa–Yadé domain, Central African Fold Belt: Implications for Western Gondwana dynamics", *Precambr. Res.* **380** (2022), article no. 106840.

Liégeois, J. P., R. Black, J. Navez and L. Latouche, "Early and late Pan-African orogenies in the Aïr assembly of terranes (Tuareg shield, Niger)", *Precambr. Res.* **67** (1994), pp. 59–88.

Maluski, H., C. Coulon, M. Popoff and P. Baudin, "$^{40}Ar/^{39}Ar$ chronology, petrology and geodynamic setting of Mesozoic to early Cenozoic magmatism from the Benue Trough, Nigeria", *J. Geol. Soc.* **152** (1995), pp. 311–326.

Maniar, P. D. and P. M. Piccoli, "Tectonic discrimination of granitoids", *Geol. Soc. Am. Bull.* **101** (1989), pp. 635–643.

Martin, H., R. H. Smithies, R. Rapp, J. F. Moyen and D. Champion, "An overview of adakite, tonalite-Trondhjemite-Granodiorite (TTG), and sanukitoid: relationships and some implications for crustal evolution", *Lithos* **79** (2005), no. 1, pp. 1–24.

Mendes, J. C., S. R. De Medeiros, I. McReath and C. M. Pinheiro de Campos, "Cambro-Ordovician Magmatism in SE Brazil: U–Pb and Rb–Sr Ages, Combined with Sr and Nd Isotopic Data of Charnockitic Rocks from the Varzea Alegre Complex", *Gondwana Res.* **8** (2005), no. 3, pp. 337–345.

Middlemost, E. A. K., "Naming material in the magma/igneous rock system", *Earth Sci. Rev.* **37** (1994), pp. 215–224.

Montes-Lauer, C. R., R. Trompette, A. J. Melfi, et al., "Pan-African Rb–Sr isochron of magmatic rocks from northern Cameroon. Preliminary results", in *Paper presented at 9th South American Symposium on isotopic geology, Brazil*, 1997.

Moreau, C., T. Regnoult, B. Déruelle and B. Robineau, "A new tectonic model for the Cameroon Line, central Africa", *Tectonophysics* **139** (1987), pp. 317–334.

Mulch, A., M. A. Cosca and M. R. Handy, "In-situ UV-laser $^{40}Ar/^{39}Ar$ geochronology of micaceous mylonite: an example of defect-enhanced argon loss", *Contrib. Miner. Petrol.* **142** (2002), pp. 738–752.

Nascimento, M. A. L., A. C. Galindo and V. C. Medeiros, "Ediacaran to Cambrian Magmatic Suites in the Rio Grande Do Norte Domain, Extreme Northeastern Borborema Province (NE of Brazil): Current Knowledge", *J. S. Am. Earth Sci.* **58** (2015), pp. 281–299.

Neves, S. P., J. M. R. Silva and O. Bruguier, "The transition zone between the Pernambuco-Alagoas Domain and the Sergipano Belt (Borborema Province, NE Brazil): geochronological constraints on the ages of deposition, tectonic setting and metamorphism of metasedimentary rocks", *J. S. Am. Earth Sci.* **72** (2016), pp. 266–278.

Ngako, V., P. Affaton and E. Njonfang, "Pan-African tectonics in northern Cameroun: implication for the history of western Gondwana", *Gondwana Res.* **14** (2008), pp. 509–522.

Ngako, V., P. Affaton, J. M. Nnangue and T. Njanko, "Pan-African tectonic evolution in central and southern Cameroon: transpression and transtension during sinistral shear movements", *J. Afr. Earth Sci.* **36** (2003), pp. 207–214.

Ngako, V. and E. Njonfang, "Plates amalgamation and plate destruction, the Western Gondwana history", in *Tectonics* (Closson, D., ed.), Intech: London, 2011, pp. 1–36. ISBN: 978-953-307-545-7.

Nkono, C., O. Féménias and D. Demaiffe, "Geodynamic framework of large volcanic fields highlighted by SRTM DEMs: Method, evaluation and perspectives exampled on three areas from the Cameroon Volcanic Line", *J. Volc. Geotherm. Res.* **187** (2009), no. 1–2, pp. 13–25.

Nkouandou, O. F., I. Ngounouno, B. Déruelle, D. Ohnenstetter, R. Montigny and D. Demaiffe, "Petrology of the Mio-Pliocene volcanism to the North and East of Ngaoundéré (Adamawa, Cameroon)", *C. R. Géosci.* **340** (2008), pp. 28–37.

Nsifa Nkonguin, E., R. Tchameni, A. Nédélec, R. Siqueira, A. Pouclet and J. Bascou, "Structure and petrology of Pan-African nepheline syenites from the South West Cameroon; Implications for their emplacement mode, petrogenesis and geodynamic significance", *J. Afr. Earth Sci.* **87** (2013), pp. 44–58.

Oliveira, E. P., S. F. Toteu, M. N. C. Araujo, M. J. Carvalho, R. S. Nascimento, J. F. Bueno, N. McNaughton and G. Basilici, "Geologic correlation between the Neoproterozoic Sergipano belt (NE Brazil) and the Yaounde belt (Cameroon, Africa)", *J. Afr. Earth Sci.* **44** (2006), pp. 470–478.

Owona, S., J. Mvondo Ondoa and G. E. Ekodeck, "Evidence of quartz, feldspar and amphibole crystal plastic deformations in the Palaeoproterozoic Nyong complex shear zones under amphibolite to granulite conditions (West Central African Fold Belt, SW Cameroon)", *J. Geog. Geol.* **5** (2013), no. 3, pp. 186–201.

Penaye, J., S. F. Toteu, A. Michard, J. M. Bertrand and D. Dautel, "Reliques granulitiques d'âge protérozoïque inférieur dans la zone mobile panafricaine d'Afrique centrale au Cameroun ; géochronologie U–Pb sur zircons", *C. R. Acad. Sci.* **309** (1989), pp. 315–318.

Philpotts, A. R. and J. J. Ague, *Principles of Igneous and Metamorphic Petrology*, 2nd edition, Cambridge University Press: New York, 2010, p. 645. ISBN 978-0-0521-88006-0.

Pickersgill, A. E., D. F. Mark, M. R. Lee and G. R. Osinski, "$^{40}Ar/^{39}Ar$ systematics of melt lithologies and target rocks from the Gow Lake impact structure, Canada", *Geochim. Cosmochim. Acta* **274** (2020), pp. 317–332.

Rickwood, P. C., "Boundary lines within petrologic diagrams which use oxides of major and minor elements", *Lithos* **22** (1989), pp. 247–264.

Saha-Fouotsa, A. N., O. Vanderhaeghe, P. Barbey, A. Eglinger, R. Tchameni, A. Zeh, P. F. Tchunte and N. Nomo Negue, "The geologic record of the exhumed root of the Central African Orogenic Belt in the central Cameroon domain (Mbé – Sassa–Mbersi region)", *J. Afr. Earth Sci.* **151** (2019), pp. 286–314.

Shellnutt, J. G., N. H. T. Pham, M.-W. Yeh and T.-Y. Lee, "Two series of Ediacaran collision-related granites in the Guéra Massif, South-Central Chad: Tectonomagmatic constraints on the terminal collision of the eastern Central African Orogenic Belt", *Precambr. Res.* **347** (2020), article no. 105823.

Solé, J., "In situ determination of K–Ar ages from minerals and rocks using simultaneous laser induced plasma spectroscopy and noble gas mass spectrometry", *Chem. Geol.* **388** (2014), pp. 9–22.

Solé, J., "An Automated System for Measuring in Situ K–Ar Ages", *Geostand. Geoanal. Res.* **45** (2021), no. 4, pp. 659–678.

Tanko Njosseu, E.L, J. P. Nzenti, T. Njanko, B. Kapajika and A. Nédélec, "New U–Pb Zircon Ages from Tonga (Cameroon): Coexisting Eburnean–Transamazonian (2.1 Ga) and Pan-African (0.6 Ga) Imprints", *C. R. Géosci.* **337** (2005), pp. 551–562.

Tchameni, R., A. Pouclet, J. Penaye, A. A. Ganwa and S. F. Toteu, "Petrography and geochemistry of the Ngaoundéré Pan-African granitoids in Central North Cameroon: Implications for sources and geological setting", *J. Afr. Earth Sci.* **44** (2006), pp. 511–529.

Tchouankoué, J.-P., N. A. Simeni Wambo, A. Kagou Dongmo and X. H. Li, "$^{40}Ar/^{39}Ar$ dating of basaltic dykes swarm in western Cameroon: evidence of Late Palaeozoic and Mesozoic magmatism in the corridor of the Cameroon Line", *J. Afr. Earth Sci.* **93** (2014), pp. 14–22.

Teixeira, M. L. A., *Integração de dados aerogeofísicos, geológicos e isotópicos do limite norte do Complexo Tamboril Santa Quitéria- CE (Província Borborema)*, MSc. Dissertation, Universidade de Brasília: Brasilia-DF, 2005. p. 91.

Tempier, P., M. Lasserre and G. Sabourdy, "Les granitoïdes du Nord Cameroun; Pétrographie et géochimie", *Bull. Soc. Géol. France* **S7-XXIII** (1981), no. 6, pp. 679–688.

Tiabou, F. A., R. Temdjim, P. Wandji, J.-M. Bardintzeff, C. V. Bih, B. T. E. Ekatah, C. N. Ngwa and O. F. X. Mebara, "Baossi–Warack monogenetic volcanoes, Adamawa Plateau, Cameroon: petrography, mineralogy and geochemistry", *Acta Geochim.* **38** (2018), pp. 40–67.

Toteu, S. F., M. J. De Wit, J. Penaye, et al., "Geochronology and correlations in the Central African Fold Belt along the northern edge of the Congo Craton: New insights from U–Pb dating of zircons from Cameroon, Central African Republic, and southwestern Chad", *Gondwana Res.* **107** (2022), pp. 296–324.

Toteu, S. F., A. Michard, J. Macaudière, J. M. Bertrand and J. Penaye, "Données géochronologiques nouvelles (U–Pb et Rb/Sr) sur la

zone mobile panafricaine du Nord Cameroun", *C. R Acad. Sci. Paris, II* **303** (1986), pp. 375–378.

Toteu, S. F., J. Penaye and Y. Poudjom Djomani, "Geodynamic evolution of the Pan-African belt in central Africa with special reference to Cameroon", *Can. J. Earth Sci.* **41** (2004), pp. 73–85.

Toteu, S. F., W. R. Van Schmus, J. Penaye and A. Michard, "New U–Pb and Sm–Nd data from north-central Cameroon and its bearing on the pre-Pan African history of central Africa", *Precambr. Res.* **108** (2001), pp. 45–73.

Valeriano, C. de M., M. Tupinambá, A. Simonetti, M. Heilbron, J. C. Horta de Almeida and L. Guilherme do Eirado, "U–Pb LA–MC–ICPMS geochronology of Cambro-Ordovician post-collisional granites of the Ribeira belt, southeast Brazil: Terminal Brasiliano magmatism in central Gondwana supercontinent", *J. S. Am. Earth Sci.* **32** (2011), pp. 416–428.

Wang, Q., F. McDermott, J. F. Xu, H. Bellon and Y. T. Zhu, "Cenozoic K-rich adakitic volcanic rocks in the Hohxil area, northern Tibet: lower crustal melting in an intra-continental setting", *Geology* **33** (2005), pp. 464–468.